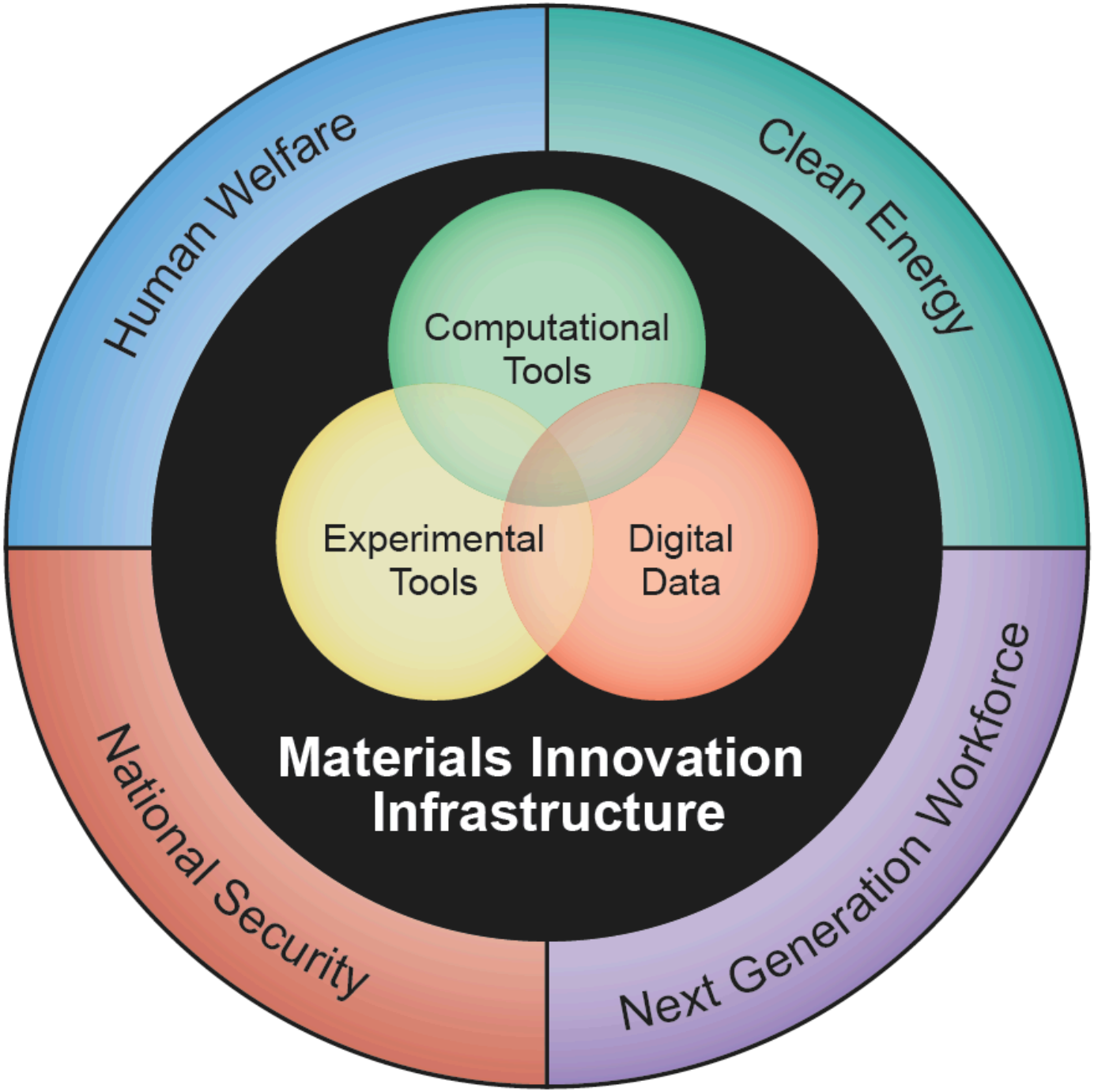
Human Welfare
Clean Energy
Computational Tools
Experimental Tools
Digital Data
Materials Innovation Infrastructure
National Security
Next Generation Workforce

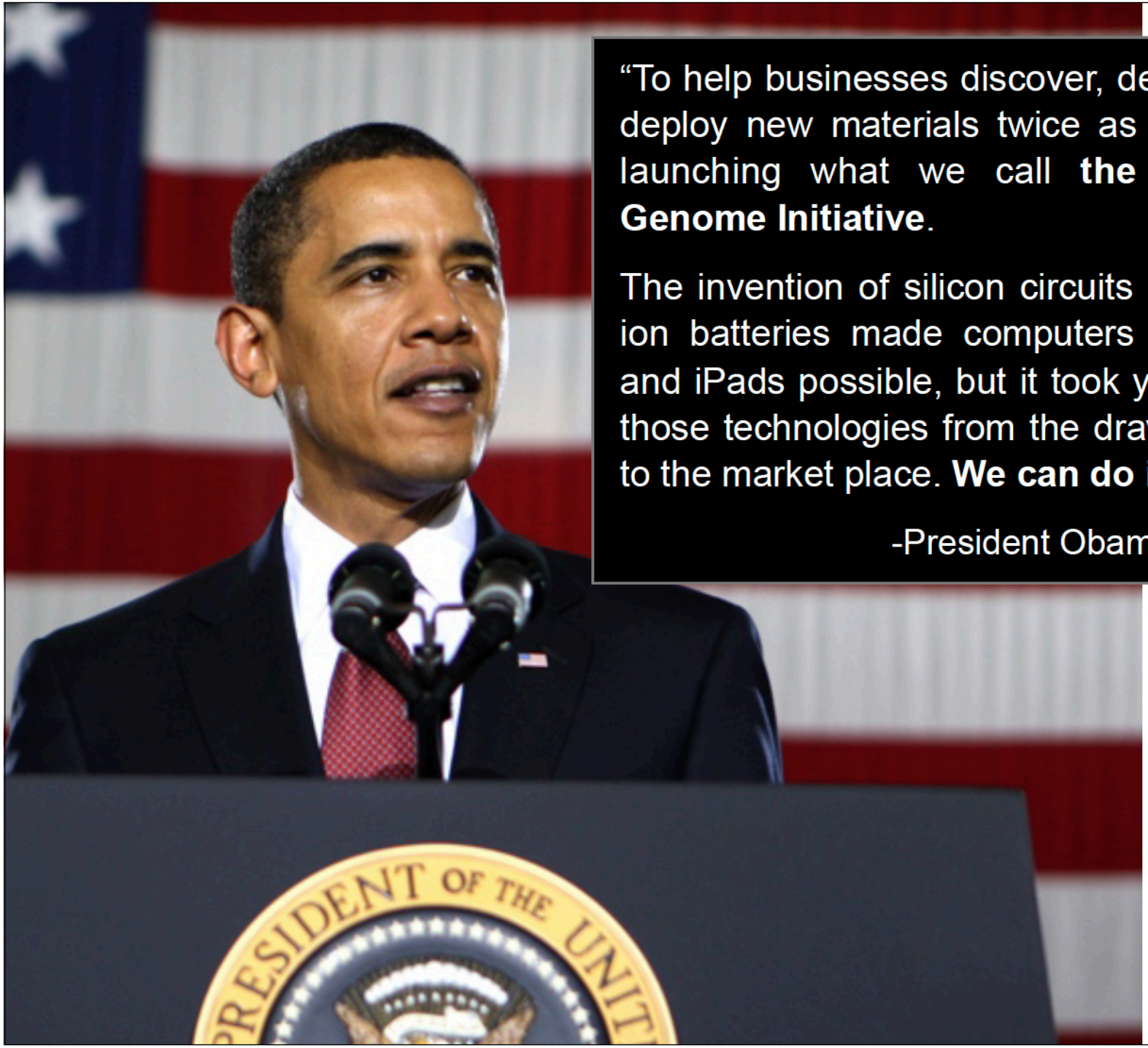

"To help businesses discover, develop, and deploy new materials twice as fast, we're launching what we call **the Materials Genome Initiative**.

The invention of silicon circuits and lithium ion batteries made computers and iPods and iPads possible, but it took years to get those technologies from the drawing board to the market place. **We can do it faster.**"

-President Obama (6/11)

What is HT computational materials

procedures of synthesis. Is there another way? Indeed, this is the burgeoning area of computational materials science called 'high-throughput' (HT) computational materials design. It is based on the marriage between computational quantum-mechanical–thermodynamic approaches[1,2] and a multitude of techniques rooted in database construction and intelligent data mining[3]. The concept is simple yet powerful: create a large database containing the calculated thermodynamic and electronic properties of existing and hypothetical materials, and then intelligently interrogate the database in the search of materials with the desired properties. Clearly, the entire construct should be validated by reality, namely the existing materials must be predicted correctly and the hypothetical ones

nature materials

REVIEW ARTICLE

PUBLISHED ONLINE: 20 FEBRUARY 2013 | DOI: 10.1038/NMAT3568

The high-throughput highway to computational materials design

Curtarolo*, Hart, Buongiorno Nardelli, Mingo, Sanvito, Levy

DOI: 10.1038/NMAT3568 (March 2013)

COMPUTATIONAL high-throughput

The practical implementation of computational HT is highly non-trivial. The method is employed in three strictly connected steps: (i) virtual materials growth: thermodynamic and electronic structure calculations of materials[3,23]; (ii) rational materials storage: systematic storage of the information in database repositories[24,25]; (iii) materials characterization and selection: data analysis aimed at selecting novel materials or gaining new physical insights[15,19,26].

Volume, Variety, Velocity, Veracity

nature materials

REVIEW ARTICLE

PUBLISHED ONLINE: 20 FEBRUARY 2013 | DOI: 10.1038/NMAT3568

The high-throughput highway to computational materials design

Curtarolo*, Hart, Buongiorno Nardelli, Mingo, Sanvito, Levy

DOI: 10.1038/NMAT3568 (March 2013)

MATERIALS GENOME: genes+descriptors

Table 1 | Examples of descriptors introduced in the literature. Nature Mater. **12**, 191 (2013)

Problem	Combination of materials properties (gene)	Descriptor
Structure stability: convex hull of an alloy system	Formation enthalpy (H_f) as a function of concentration (x) and the enthalpies (H) of A and B.	$H_f(x) = H(A_{1-x}B_x) - (1-x)H(A) - xH(B)$
Phase stability in off-lattice alloys PR	Spectral decomposition of alloy vector-energies (E_{np}, n-rows = species, p-columns = c alysis coefficients (a	$E_{np} \approx \alpha_1 E_{np} + \dots + \alpha_n E_{np} + \epsilon(d)$
Nano PR	Ratio of the av) (ref. 15).	
Topol Natu	Variational rat rbit derivative stra at k, a_0 lattice)[16].	
Powe (spectroscopic limited maximum efficiency) PRL **108**, 068701 (2012)	Ratio of the m ident solar energy density (P_{in}) — a function (η) of the radiative electron–hole recombination current (f_r) and the photon absorptivity ($\alpha(E)$) — versus bandgap energy (E_g)[62].	$\eta(\alpha(E), f_r) = P_m/P_{in}; E_g$
Non-proportionality in scintillators IEEE Trans. Nucl. Sci. **56**, 2989 (2009)	Maximum mismatch between effective masses of electrons (m_e) and holes (m_h)[75].	$\hat{\chi}_{np} \equiv \max\left(\frac{m_e}{m_h}, \frac{m_h}{m_e}\right)$
Morphotropic phase boundary piezoelectrics PRB **84**, 014103 (2011)	Energy proximity between tetragonal, rhombohedra and rotational distortions (ΔE_p). Angular coordinate (α_{AB}) of the energy minimum in the A–B off-centerings energy map for ABO_3 systems[79].	$\Delta E_p \leq 0.5$ eV $\alpha_{AB} \approx 45°$

the "problem"

qualitative picture

quantitative picture

The automatism is all about creating a big picture from many small details

Lycurgus cup (290~325 AD) AgAu NP~10nm
dichroism by resonant surface plasmon

AFLOWLIB.org: a materials properties repository from HT calculations

AFLOW framework libraries: www.aflowlib.org
Online/socket commands for the SQL database interrogation.
Distributed platform (Linux/UNIX)

(a)

AFLOWLIB.ORG

CHOOSE DATABASES

☑ AFLOWLib ☑ Structure Properties ☐ Electronic Properties ☐ Thermoelectric Properties ☐ Scintillator Database ☑ Magnetic Properties ☐ Job Status

SEARCH AFLOWLIB (379,310 Compounds)
(188,768 Heusler Alloys; 173,324 Binary Alloys; 17,218 ICSD Compounds)

Element(s) Al & Mn & Ni — *Usage:* &(and), |(or), ~(not), ^(xor), m(metal) *e.g. ~Si and Al: having Al but not Si*

Species number 3

Prototype Heusler (AlCu2Mn)

Space Group Number — Pearson Symbol — (structure properties)

Minimum band gap = 0 eV — Maximum band gap = 17.506 eV — (electronic properties)

Band Gap Type All types — (electronic properties)

Minimum $\langle P_n \rangle / L$ = 0.00 μW/cmK²nm — Maximum $\langle P_n \rangle / L$ = 16025.65 μW/cmK²nm — (thermoelectric properties)

Minimum $\langle P_p \rangle / L$ = 0.00 μW/cmK²nm — Maximum $\langle P_p \rangle / L$ = 34373.53 μW/cmK²nm — (thermoelectric properties)

Minimum magnetic moment = 0.00 μ_B/atom — Maximum magnetic moment = 223.99 μ_B/atom — (magnetic properties)

Minimum $\Delta S(E_F)$ = 0.00 — Maximum $\Delta S(E_F)$ = 1.00 — (magnetic properties)

AFlow version from 299523 to 30427 — Calculated date from 2009-10-07 to 2012-07-31 — (Job status)

(b)

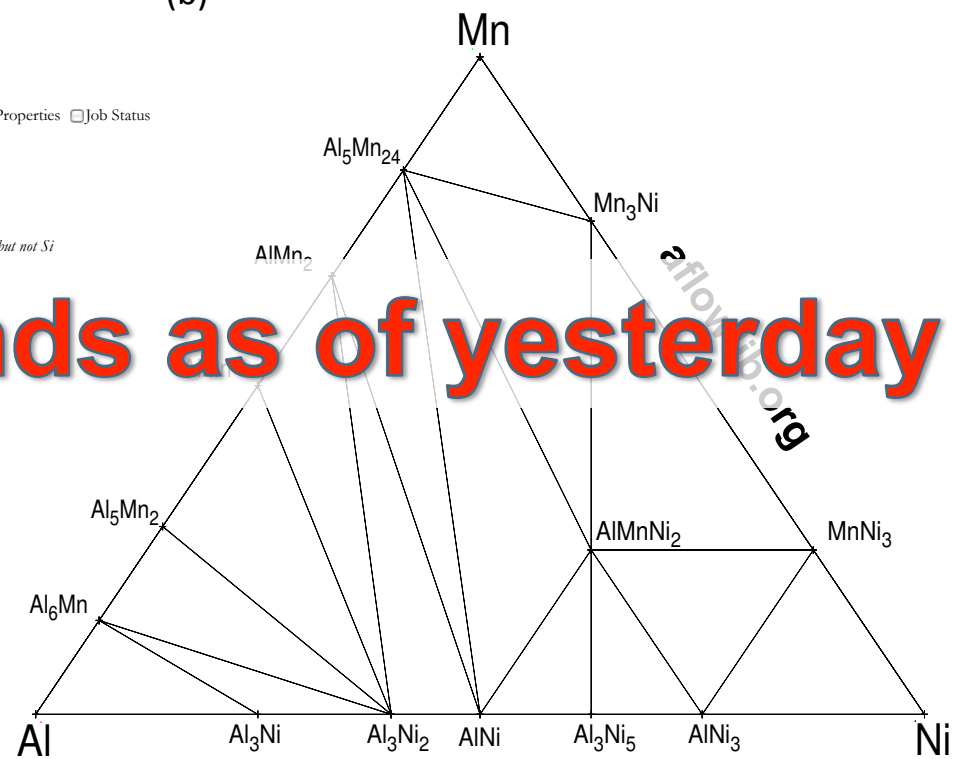

500,000 compounds as of yesterday

Curtarolo, Hart, Buongiorno Nardelli, et al. AFLOWLIB: a materials properties repository from HT calculations, Comp. Mat. Sci. **58**, 227 (2012)

$Al_1Ca_1O_5Ta_1$ (ICSD# 99001)

Real Space Lattices

Lattices:	a = 7.40Å b = 7.97Å c = 7.71Å α = 68.69° β = 90.00° γ = 90.00°
Volume:	423.76Å^3
Unit Cell Atom Number:	32
Space Group Number:	14
Pearson Symbol:	mP32
Lattice Primitive:	MCL Al1Ca1O5Ta1 #14.0 - (Al1Ca1O5Ta1_ICSD_99
Lattice Variation:	MCL
Crystal Family:	Monoclinic
Crystal System:	Monoclinic
Crystal Class:	Monoclinic-prismatic
Point Group (Hermann Mauguin):	2/m PGXTAL
Point Group (Schoenflies):	C_2h
Point Group Orbifold:	2*
Point Group Type:	centrosymmetric
Point Group Order:	4
Point Group Structure:	2 X Cyclic
Superlattice Primitive unit cell:	MCL
Superlattice Variation:	MCL
Pearson Symbol Superlattice:	mP32

P 1 [P 1]
a=7.399Å
b=7.971Å
c=7.713Å
α=68.7°
β=90.0°
γ=90.0°

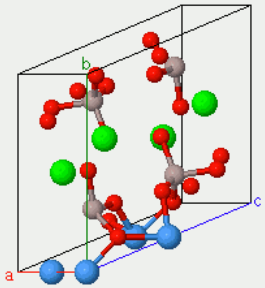

☑ Turn spin off

☐ Show atom labels

ball and stick

Density:	5.45 g/cm^3
Band Gap:	2.68 eV
Fit Band Gap:	4.53 eV
Band Gap Type:	Indirect
Electron Mass:	6.66 (m_0)
Hole Mass:	2.85 (m_0)

Reciprocal Space Lattices

Reciprocal Lattices:	a = 0.85Å b = 0.85Å c = 0.87Å α = 111.31° β = 90.00° γ = 90.00°
Volume:	0.59 Å^{-3}
Lattice Primitive:	MCL
Lattice Variation:	MCL

Electronic Properties

Band Structure

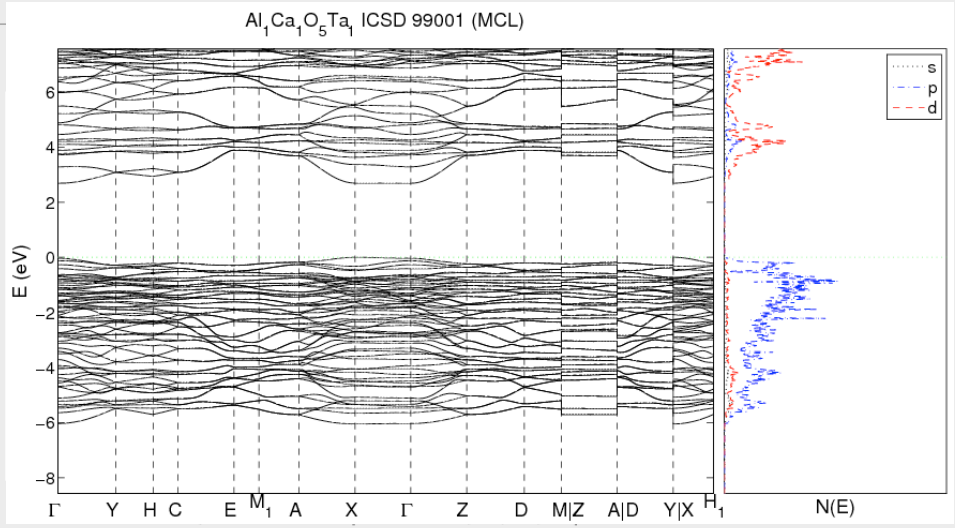

MCL path: Γ-Y-H-C-E-M_1-A-X-Γ-Z-D-M|Z-A|D-Y|X-H_1

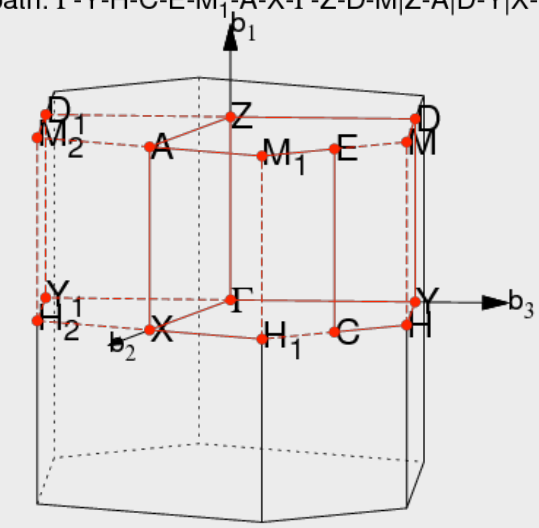

Repository of quantum mechanics calculations

geometrical structural data (with formation energies ☺)

thermoelectric data (power factors etc.)

▲Name [1]	ICSD Number [1]	Bravais Lattice	Number of Atoms	<Pn>/L (μW/cmK²nm) [4]	<Pn1>/L (μW/cmK²nm) [4]	<Pn2>/L (μW/cmK²nm) [4]	<Pn3>/L (μW/cmK²nm) [4]	<Pp>/L (μW/cmK²nm) [4]	<Pp1>/L (μW/cmK²nm) [4]	<Pp2>/L (μW/cmK²nm) [4]	<Pp3>/L (μW/cmK²nm) [4]	Sn (μV/K) [4]	Sp (μV/K) [4]
$F_3Fe_1K_1$	15424	CUB (Cubic)	5	0.15	0.15	0.15	0.15	2.17	2.17	2.17	2.17	-116.36	91.29
$F_3Fe_1Rb_1$	49586	CUB (Cubic)	5	0.24	0.24	0.24	0.24	1.50	1.48	1.51	1.51	-91.73	91.04
$Fe_1La_1O_3$	29118	CUB (Cubic)	5	0.31	0.31	0.31	0.31	2.00	2.00	2.00	2.00	-139.02	92.92
$Ag_2Fe_1S_4Sn_1$	42534	BCT (Tetragonal)	8	121 (I-42m)	tI16	4.77							

magnetic properties (if you want rare-earth-free magnets/spintronics)

scintillation properties/search

▲Name [1]	ICSD Number [1]	Bravais Lattice	Number of Atoms	Magnetic Moment (μB/atom) [5]	Spin Polarization (1/atom) [5]	Spin Decomposition (μB)
$Ag_1Fe_1O_2$	2786	HEX (Hexagonal)	8	1.25	0.00	{0.039,0.039,4.303,4.303,0.258,0.258,0.258,0.258}
$Ag_1Fe_1O_2$	31919	RHL (Rhombohedral)	4	1.25	0.00	{0.039,4.303,0.258,0.258}
$Ag_2Fe_1S_4Sn_1$	42534	BCT (Tetragonal)	8	0.50	0.00	{0.016,0.016,3.631,0.024,0.024,0.024,0.024,0.016}
F_2Fe_1	9166	TET (Tetragonal)	6	2.63 (I)	4.46	0.49	0.48	190.80	5.47	388.39	7.15	15.23	2.86700

Curtarolo, Hart, Buongiorno Nardelli, et al. AFLOWLIB: a materials properties repository from HT calculations, Comp. Mat. Sci. **58**, 227 (2012)

Automatic Generation of Databases

Creating “aflow.in” input files:

```
kesong@beta:/tmp$
```

HT Computational Tools (AFLOW)

+

DFT kernel

Materials Database (AFLOWLIB)

Curtarolo, Hart, Buongiorno Nardelli, et al. AFLOWLIB: a materials properties repository from HT calculations, Comp. Mat. Sci. **58**, 227 (2012)

integrated suite of Open-Source computer codes for electronic-structure calculations and materials modeling at the nanoscale. It is based on density-functional theory, plane waves, and pseudopotentials.

- Quantum ESPRESSO is not a monolithic application, but an integrated ecosystem thriving around a small number of core components developed and maintained by a small number of developers
- the ecosystem is designed so as to be alien-friendly: a number of third-party QE-compatible applications and add-ons, often designed to be code-agnostic, are distributed with QE (notable examples include *WanT*, *yambo*, *EPW, Wannier90, XCrysDen, ...*)
- the environment that allows the ecosystem to prosper is provided by the *qe-forge.org* platform, freely available to researchers and developers from all over the world

integrated suite of Open-Source computer codes for electronic-structure calculations and materials modeling at the nanoscale. It is based on density-functional theory, plane waves, and pseudopotentials.

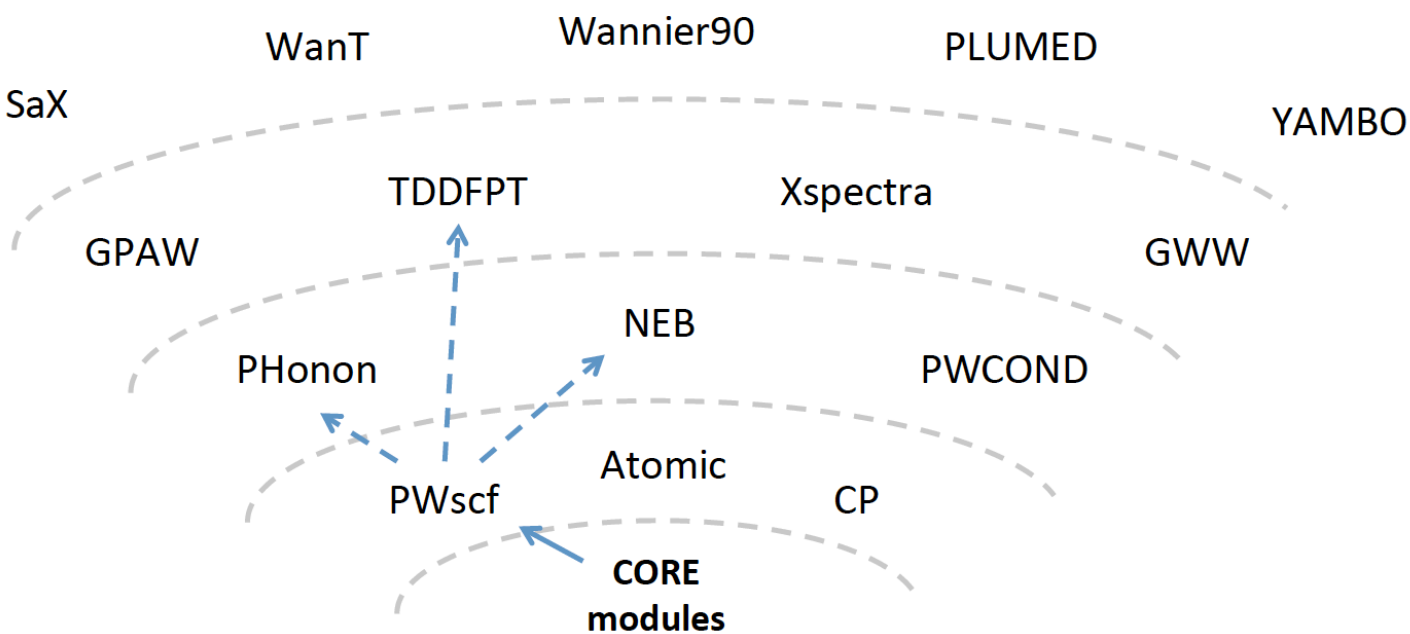

Automatic data/visualization analysis

Extract general materials properties: structural, electronic, magnetic properties…

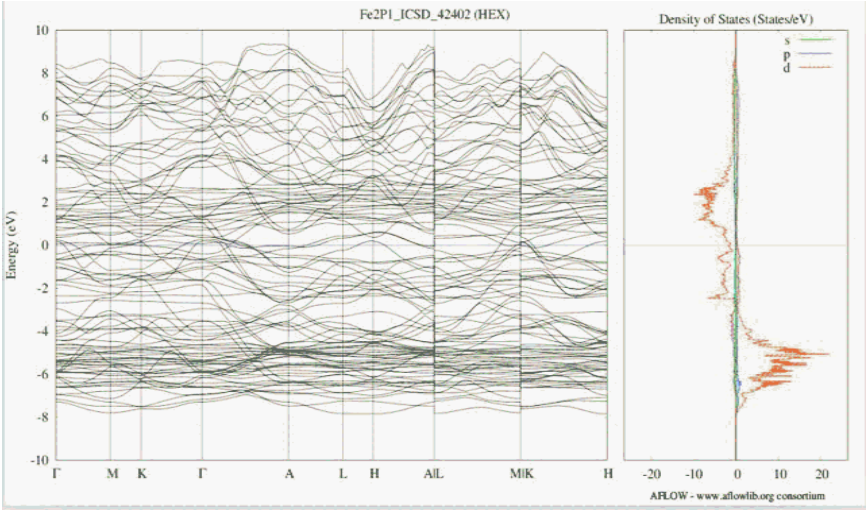

Develop new high-throughput programs based on the desired materials properties

AFLOW: an automatic framework for high-throughput materials discovery, Comp. Mat. Sci. **58**, 218-226 (2012)

The search for functionality: Topological Insulators

Table 1 | Examples of descriptors introduced in the literature. Nature Mater. **12**, 191 (2013)

Problem	Combination of materials properties (gene)	Descriptor
Structure stability: convex hull of an alloy system	Formation enthalpy (H_f) as a function of concentration (x) and the enthalpies (H) of A and B.	$H_f(x) = H(A_{1-x}B_x) - (1-x)H(A) - xH(B)$
Phase stability in off-lattice alloys PRL **91**, 135503 (2003)	Spectral decomposition of alloy vector-energies ($E_{n,p}$, n-rows = species, p-columns = configurations) with principal-component-analysis coefficients (α_i) and truncation error ($\epsilon(d)$) (ref. 3).	$E_{n,p} \simeq \alpha_1 E_{n,1} + \cdots + \alpha_{p-1} E_{n,p-1} + \epsilon(d)$
Nanosintered thermoelectrics PRX **1**, 021012 (2011)	Ratio of the average power factor ($<P>$) to the grain size (L) (ref. 15).	$\hat{\chi}_{\text{thermo}} \equiv \frac{<P>}{L}$
Topological insulators (epitaxial growth) Nature Mater. **11**, 614 (2012)	Variational ratio of spin–orbit distortion versus non-spin–orbit derivative strain (E_k^{SOC}, E_k^{noSOC}, spin/no spin–orbit bandgaps at k, a_0 lattice)[16].	$\hat{\chi}_{\text{TI}} \equiv -\frac{E_k^{SOC}(a_0)/a_0}{\delta E_k^{noSOC}(a)_0/\delta a_0\big\vert_{a_0}}$
Power conversion efficiency of a solar cell (spectroscopic limited maximum efficiency) PRL **108**, 068701 (2012)	Ratio of the maximum output power density (P_m) to the incident solar energy density (P_{in}) — a function (η) of the radiative electron–hole recombination current (f_r) and the photon absorptivity ($\alpha(E)$) — versus bandgap energy (E_g)[62].	$\eta(\alpha(E), f_r) = P_m/P_{in}; E_g$
Non-proportionality in scintillators IEEE Trans. Nucl. Sci. **56**, 2989 (2009)	Maximum mismatch between effective masses of electrons (m_e) and holes (m_h)[75].	$\hat{\chi}_{np} \equiv \max\left(\frac{m_e}{m_h}, \frac{m_h}{m_e}\right)$
Morphotropic phase boundary piezoelectrics PRB **84**, 014103 (2011)	Energy proximity between tetragonal, rhombohedra and rotational distortions (ΔE_p). Angular coordinate (α_{AB}) of the energy minimum in the A–B off-centerings energy map for ABO_3 systems[79].	$\Delta E_p \leq 0.5$ eV $\alpha_{AB} \approx 45°$

The search for functionality: Topological Insulators

- An insulator has an energy gap separating filled and empty bands of electronic states – transparent if gap is large enough
- Quantum Hall state – 2D gas in magnetic field:
  - Bulk: an energy gap results from the quantization of the closed circular orbits that electrons follow in a magnetic field.
  - Edges: unique states where charge can flow in one direction only – insensitive to scattering
- Quantum Spin Hall state – electrons of different spin move in opposite directions in protected states created by the interaction of the spin magnetic moment with the electron orbital moment (spin-orbit coupling)

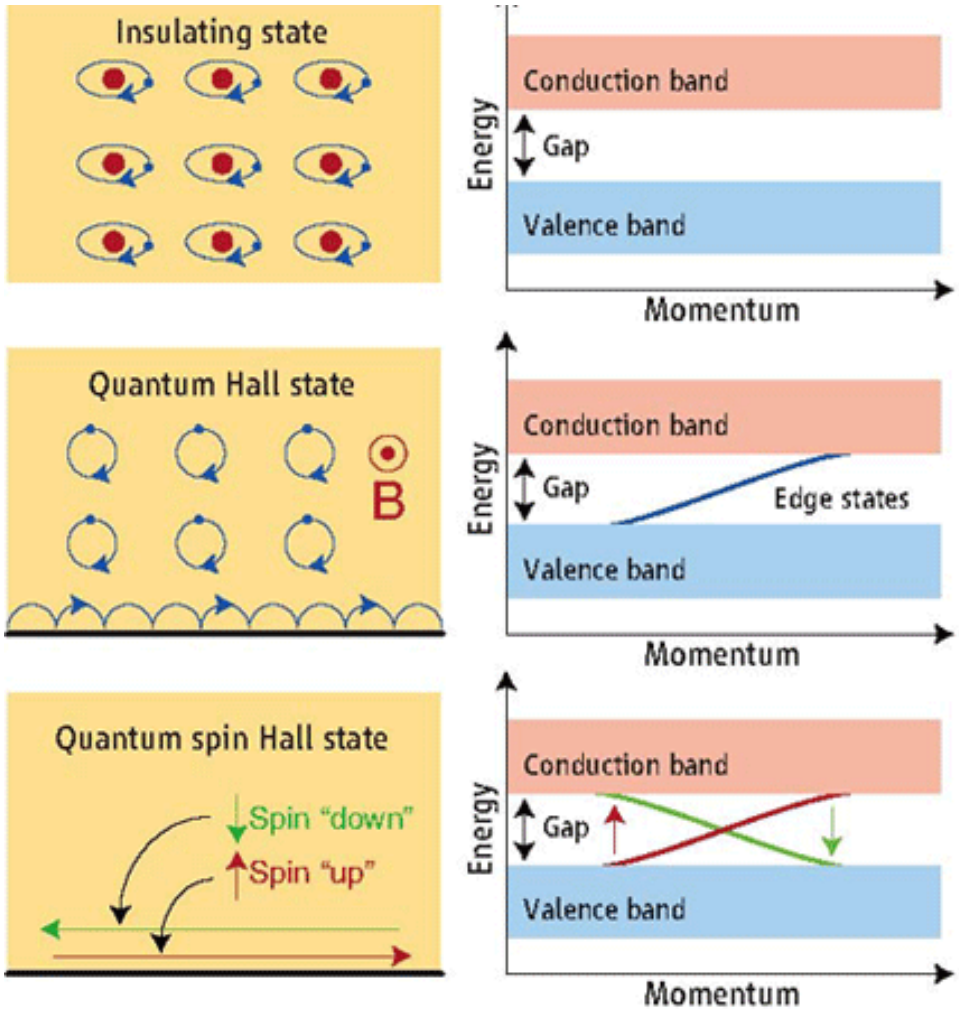

Example: a plan of action

- Scan the aflowlib.org library
- Need of a **DESCRIPTOR (need to grow… epixially).**
- search for combination of heavy metals (potential strong spin-orbit coupling)
- search for ideal band structures with appropriate gaps
- calculate band structure with LS (thousand of compounds)
- calculate the bands for surfaces to see localized conducting surface stares
- usually they contain Bi and/or Sb,Te, Pb.

Time Reversal Invariant Momenta (TRIMs)

$$\Gamma_{i=(n_1 n_2 n_3)} = (n_1 \mathbf{b}_1 + n_2 \mathbf{b}_2 + n_3 \mathbf{b}_3)/2, \quad \text{with} \quad n_j = 0, \quad 1.$$

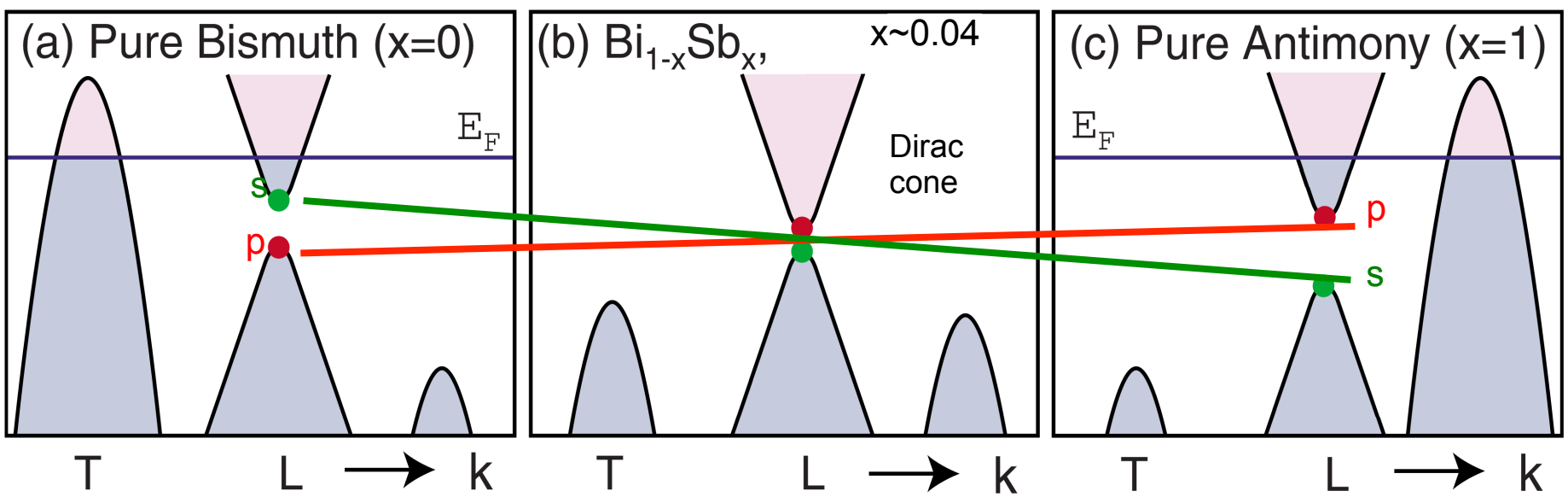

Nature Materials, ***11****(7), 614-619 (2012)*

Let`s precess, epitaxially !

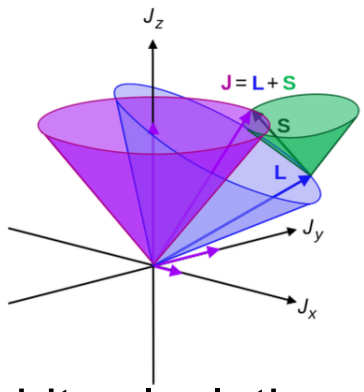

α) SPIN orbit calculations are expensive

β) LS due to electrons precessing near cores

γ) E^{soc}-E^{noSOC} ~ const

δ) simulated epitaxial strain with E^{noSOC}

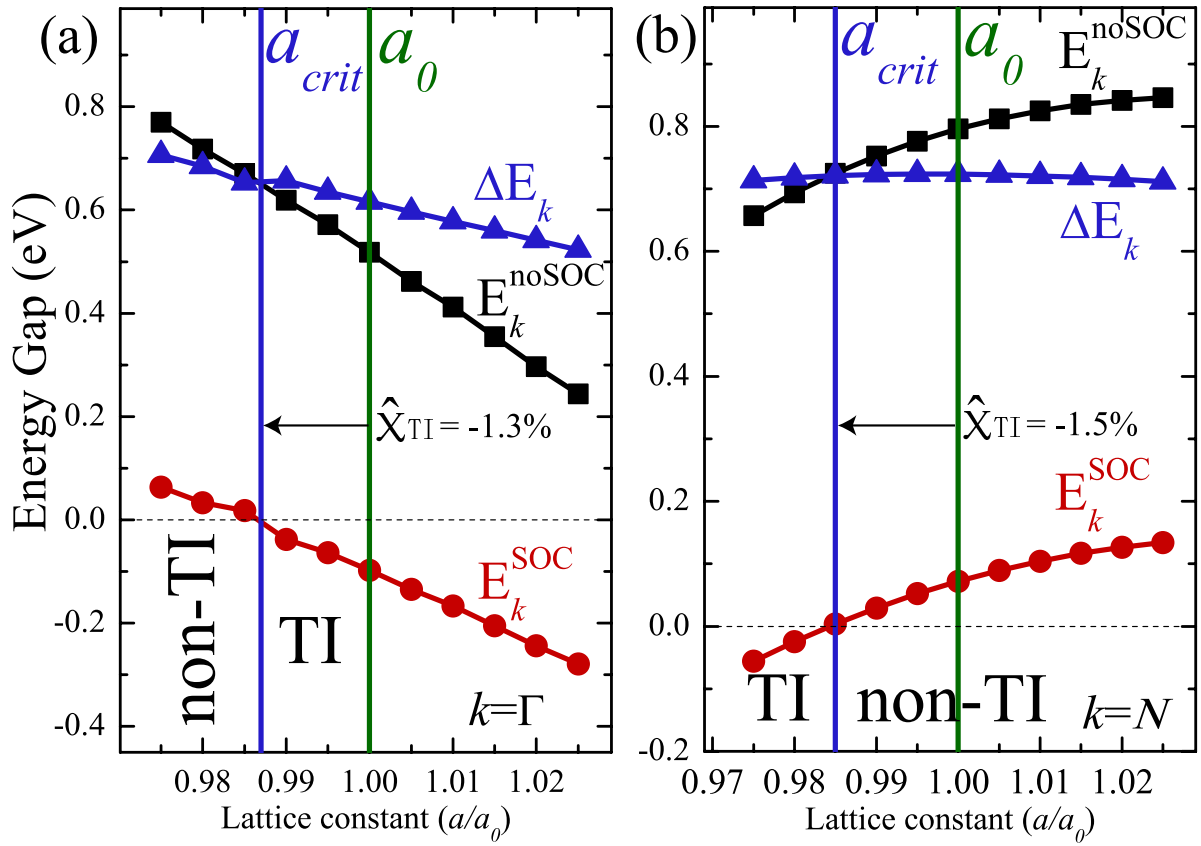

Bi_2Te_2S at $k=\Gamma$ — covalent systems

PbTe at $k=N$ — ionic compounds

robustness descriptor variational ("quasi-meaningful" quantity)

$$\hat{\chi}_{TI} \equiv -\frac{E_k^{SOC}(a_0)/a_0}{\delta E_k^{noSOC}(a)/\delta(a)\big|_{a_0}}$$

Example: a plan of action

- Scan the aflowlib.org library
- Need of a **DESCRIPTOR (need to grow… epixially).**
- search for combination of heavy metals (potential strong spin-orbit coupling)
- search for ideal band structures with appropriate gaps
- calculate band structure with LS (thousand of compounds)
- calculate the bands for surfaces to see localized conducting surface stares
- usually they contain Bi and/or Sb,Te, Pb.

nature materials

ARTICLES

PUBLISHED ONLINE: 13 MAY 2012 | DOI: 10.1038/NMAT3332

A search model for topological insulators with high-throughput robustness descriptors

Kesong Yang[1], Wahyu Setyawan[2], Shidong Wang[1], Marco Buongiorno Nardelli[3,4] and Stefano Curtarolo[1,4,5]★

Nature Materials, ***11****(7), 614-619 (2012)*

New compounds: Cs{Sn,Pb,Ge}{Cl,Br,I}$_3$

Table 1 | Properties of bulk and simulated epitaxial structures.

			Bulk				Simulated epitaxial growth (a optimized, c/a free)									
Compound	Space group	ICSD # ref. 31	Pearson symbol	Latt. ref. 39	Exp. a_0, c_0	DFT a_0, c_0	Pearson symbol	Latt. cleav.	a_{crit} (Å)	E_k^{SOC} 'ref'	Ref. lattice	E_g^{SOC} 'ref'	TRIM (mult.)	ΔE_k @ (a_0, c_0)	E_k^{SOC} @ (a_0, c_0)	$\hat{\chi}_{TI}$ (%)
Sb_2Te_2S	$R\bar{3}m$	–	hR5	rhl$_1$	–	4.192	hR5	rhl$_1$	$1.006a_0$	−0.106	$1.019a_0$	0.106	Γ (1)	0.21	0.043	0.6
						31.001		(0001)	$0.993c_0$		$0.975c_0$	(D)				PF
Bi_2Te_2S	$R\bar{3}m$	617050	hR5	rhl$_1$	4.33	4.297	hR5	rhl$_1$	$0.987a_0$	−0.089	a_0	0.089	Γ (1)	0.62	−0.089	−1.3
Fig. 2a					30.07	31.513		(0001)	$1.013c_0$		c_0	(D)				R
$SnSb_2Te_4$	$R\bar{3}m$	30392	hR7	rhl$_1$	4.312	4.389	hR7	rhl$_1$	$0.999a_0$	−0.065	$1.011a_0$	0.065	Z(1)	0.22	0.013	−0.1
					41.72	42.347		(0001)	$0.998c_0$		$0.984c_0$	(D)				PF
$PbSb_2Te_4$	$R\bar{3}m$	250250	hR7	rhl$_1$	4.35	4.413	hR7	rhl$_1$	$0.988a_0$	−0.017	a_0	0.017	Z(1)	0.35	−0.017	−1.2
					41.712	42.792		(0001)	$1.011c_0$		c_0	(D)				R
$PbBi_4Se_7$	$P\bar{3}m1$	ref. 49	hP12	hex	4.25	4.216	hP12	hex	$1.018a_0$	−0.016	$1.023a_0$	0.016	A(1)	0.41	0.128	2.3
					22.68	23.839		(0001)	$0.971c_0$		$0.966c_0$	(D)				PF
$CsSnCl_3$	$Pm\bar{3}m$	28082	cP5	cub	5.504	5.618	tP5	tet	$0.951a_0$	−0.281	$0.936a_0$	0.111	A(1)	0.34	0.646	−4.9
					5.504	5.618		(001)	$1.022c_0$		$1.209c_0$	(I)				HF
$CsPbCl_3$	$Pm\bar{3}m$	29072	cP5	cub	5.605	5.733	tP5	tet	$0.914a_0$	−0.450	$0.890a_0$	0.354	A(1)	1.11	1.073	−8.6
					5.605	5.733		(001)	$1.037c_0$		$1.050c_0$	(I)				HF
$CsGeBr_3$	$Pm\bar{3}m$	80320	cP5	cub	5.36	5.603	tP5	tet	$0.955a_0$	−0.055	$0.952a_0$	0.026	A(1)	0.16	0.591	−4.5
					5.36	5.603		(001)	$1.022c_0$		$1.023c_0$	(I)				HF
$CsSnBr_3$	$Pm\bar{3}m$	4071	cP5	cub	5.795	5.884	tP5	tet	$0.972a_0$	−0.099	$0.965a_0$	0.099	A(1)	0.34	0.288	−2.8
					5.795	5.884		(001)	$1.010c_0$		$1.013c_0$	(D)				PF
$CsPbBr_3$	$Pm\bar{3}m$	29073	cP5	cub	5.874	5.993	tP5	tet	$0.934a_0$	−0.120	$0.926a_0$	0.120	A(1)	1.11	0.641	−6.6
					5.874	5.993		(001)	$1.024c_0$		$1.027c_0$	(D)				HF
$CsSnI_3$	$Pm\bar{3}m$	69997	cP5	cub	6.219	6.272	tP5	tet	$0.993a_0$	−0.335	$0.960a_0$	0.169	A(1)	0.39	0.070	−0.7
Fig. 2d					6.219	6.272		(001)	$1.002c_0$		$1.013c_0$	(I)				PF
SnTe	$Fm\bar{3}m$	52489	cF8	fcc	4.471	4.528	tI4	bct$_2$	$1.027a_0$	−0.058	$1.010a_0$	0.058	N (4)	0.15	−0.107	2.7
					6.323	6.404		(001)	$0.998c_0$		$0.999c_0$	(D)				VR

Properties of bulk structure: compound (∗ indicates experimental validation), space group, ICSD number[31], Pearson symbol, Bravais lattice[39], experimental and DFT equilibrium lattices a, c in (Å). Properties under the simulated epitaxial growth condition: Pearson symbol, Bravais lattice with conventional cleavage Miller indices, critical value for band inversion (a_{crit}), SOC band energy difference ($E_k^{SOC}(ref.)$) at the TRIM with the reference lattice, reference lattice, SOC band-gap at the reference lattice (direct/indirect) ($E_g^{SOC}(ref.)$), TRIMs having band inversion with multiplicity[39], SOC energy-gap discrepancy (ΔE_k) at the *ab initio* equilibrium lattice, SOC band energy difference ($E_k^{SOC}(a_0)$) at the TRIM with the *ab initio* equilibrium lattice, HT-descriptor ($\hat{\chi}_{TI}$). The labels below $\hat{\chi}_{TI}$ indicate: F(fragile), R(robust), VR(very robust), PF(potentially feasible), and HF(hardly feasible) (structural and electronic data is available by following the links listed in the Supplementary Information Extended Table).

novel ternary halides

if $E_k^{SOC}(a_0) \leq 0$, **robustness**:
$|\hat{\chi}_{TI}| \leq 1\% \Rightarrow$ fragile,
$1\% < |\hat{\chi}_{TI}| \leq 2\% \Rightarrow$ robust,
$2\% < |\hat{\chi}_{TI}| \Rightarrow$ very-robust.

if $E_k^{SOC}(a_0) > 0$, **feasibility**:
$|\hat{\chi}_{TI}| \leq 3\% \Rightarrow$ potentially-feasible,
$3\% < |\hat{\chi}_{TI}| \Rightarrow$ hardly-feasible.

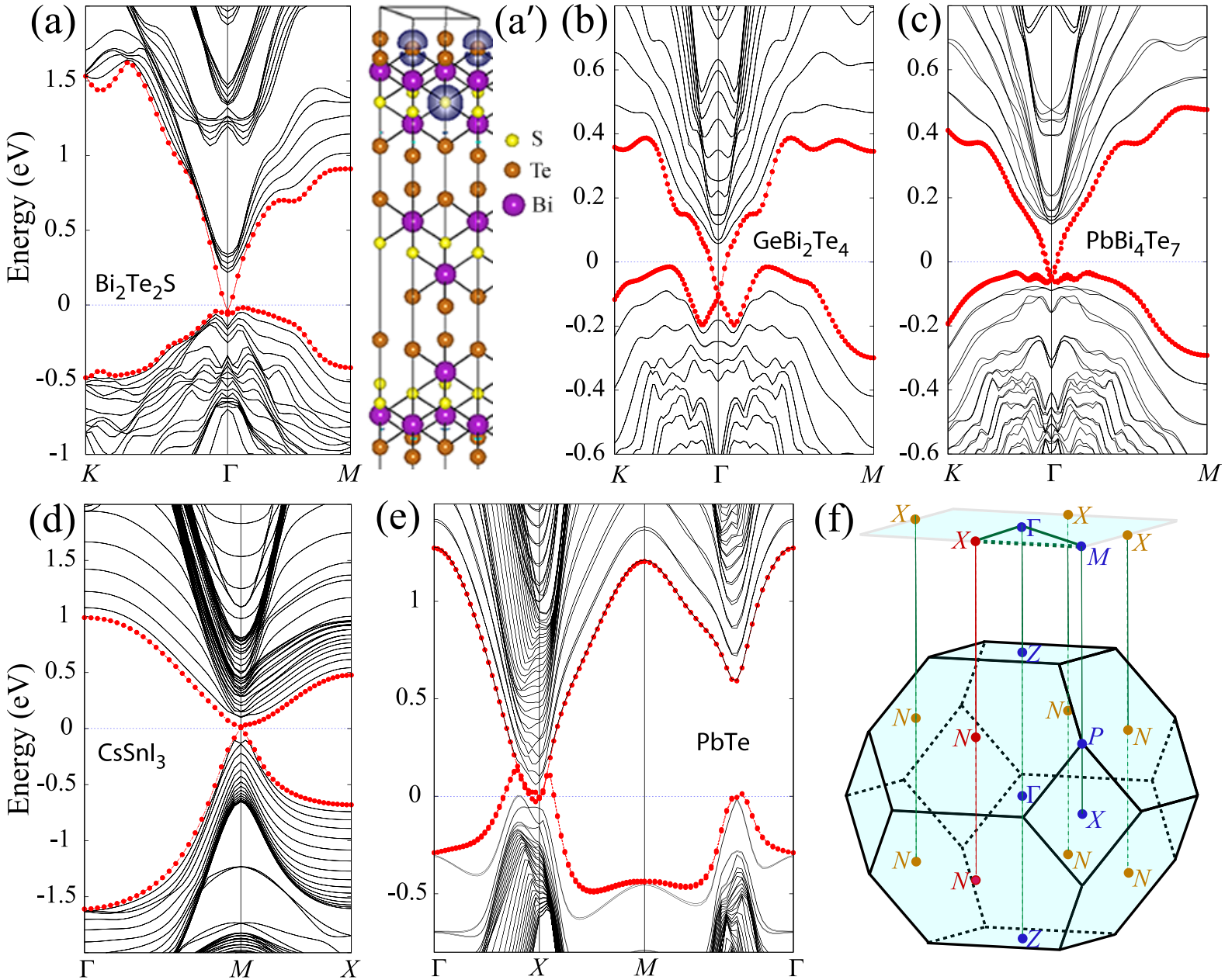
(a)
Energy (eV)
Bi_2Te_2S
K
Γ
M
(a′)
S
Te
Bi
(b)
$GeBi_2Te_4$
(c)
$PbBi_4Te_7$
(d)
$CsSnI_3$
(e)
PbTe
(f)
X
Γ
M
Z
N
P

top. insul.

TI surfaces and interfaces

Projects on surfaces by aligning semi-cones and checking thermodynamics of planes

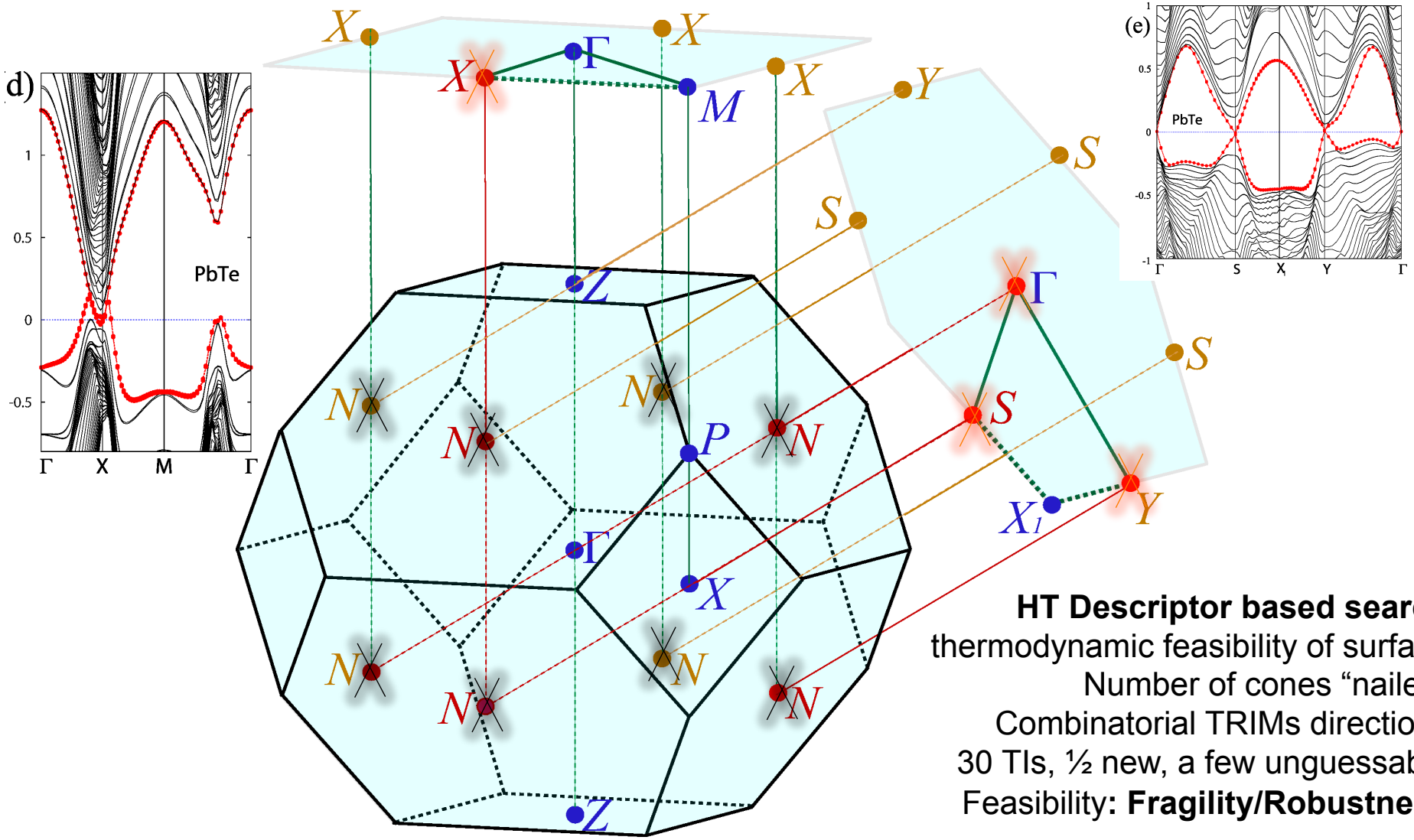

HT Descriptor based search
thermodynamic feasibility of surface
Number of cones "nailed"
Combinatorial TRIMs directions
30 TIs, ½ new, a few unguessable
Feasibility**: Fragility/Robustness**

The search for functionality: Half-Metallic Oxides

VOLUME 50, NUMBER 25 PHYSICAL REVIEW LETTERS 20 JUNE 1983

New Class of Materials: Half-Metallic Ferromagnets

R. A. de Groot and F. M. Mueller
Research Institute for Materials, Faculty of Science, Toernooiveld, 6525 ED Nijmegen, The Netherlands

and

P. G. van Engen and K. H. J. Buschow
Philips Research Laboratories, 5600 JA Eindhoven, The Netherlands

(Received 21 March 1983)

The band structure of Mn-based Heusler alloys of the $C1_b$ crystal structure (MgAgAs type) has been calculated with the augmented-spherical-wave method. Some of these magnetic compounds show unusual electronic properties. The majority-spin electrons are metallic, whereas the minority-spin electrons are semiconducting.

PACS numbers: 71.10.+x, 71.25.Pi, 75.20.En

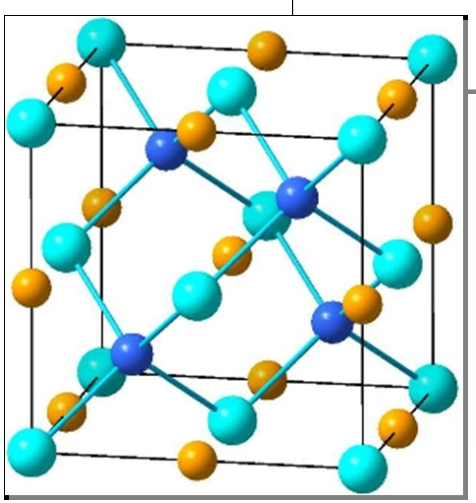

Compound	$N(E)\uparrow$	$N(E)\downarrow$	$n_{3d}^{Mn}\uparrow$	$n_{3d}^{Mn}\downarrow$	μ_{tot}^{cacl}	μ_{tot}^{exp}
NiMnSb	9.90	0	4.51	0.87	4.00	3.85
PtMnSb	10.05	0	4.57	0.79	4.00	3.97
PdMnSb	9.04	2.97	4.58	0.71	4.05	3.95
PtMnSn	9.78	19.31	4.40	0.78	3.60	3.42

The search for functionality: Half-Metallic Oxides

VOLUME 50, NUMBER 25 PHYSICAL REVIEW LETTERS 20 JUNE 1983

New Class of Materials: Half-Metallic Ferromagnets

R. A. de Groot and F. M. Mueller
Research Institute for Materials, Faculty of Science, Toernooiveld, 6525 ED Nijmegen, The Netherlands

and

[illegible]

True first principle prediction!

(Received 21 March 1983)

The band structure of Mn-based Heusler alloys of the $C1_b$ crystal structure (MgAgAs type) has been calculated with the augmented-spherical-wave method. Some of these magnetic compounds show unusual electronic properties. The majority-spin electrons are metallic, whereas the minority-spin electrons are semiconducting.

PACS numbers: 71.10.+x, 71.25.Pi, 75.20.En

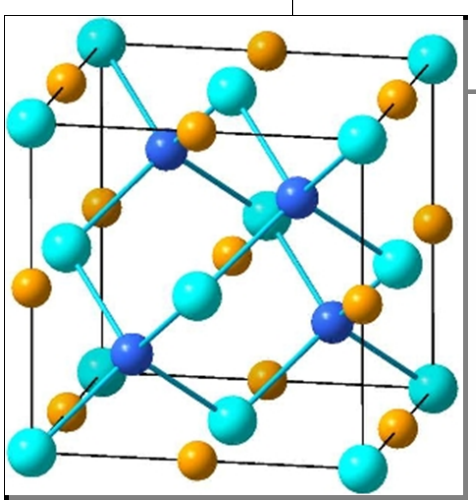

Compound	$N(E)\uparrow$	$N(E)\downarrow$	$n_{3d}^{Mn}\uparrow$	$n_{3d}^{Mn}\downarrow$	μ_{tot}^{cacl}	μ_{tot}^{exp}
NiMnSb	9.90	0	4.51	0.87	4.00	3.85
PtMnSb	10.05	0	4.57	0.79	4.00	3.97
PdMnSb	9.04	2.97	4.58	0.71	4.05	3.95
PtMnSn	9.78	19.31	4.40	0.78	3.60	3.42

The search for functionality: Half-Metallic Oxides

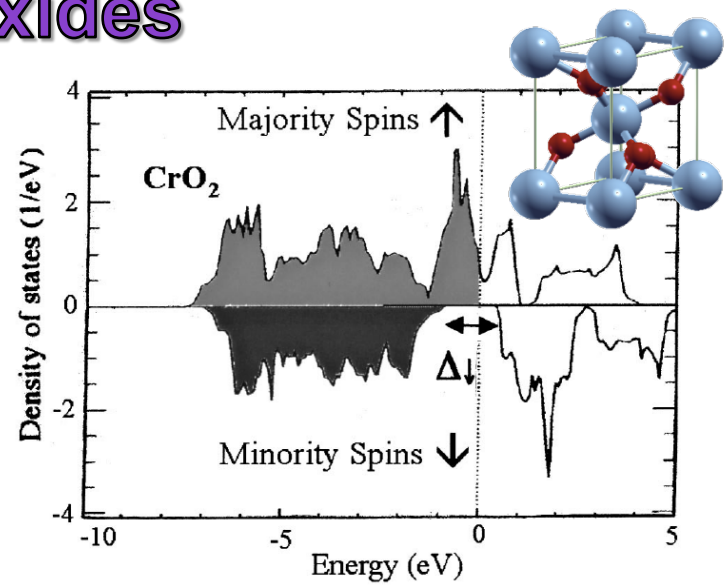

- New state of matter
  - Metallic spin up channel
  - Insulating spin-down channel
- Properties include
  - Colossal Magneto-Resistance (CMR)
  - Colossal Intergrain MR

Thin films, interfaces

- Applications
  - Ultrathin, transparent spintronic devices
    - To maximize CMR performance of layered devices
    - Spin valve devices

CrO_2-TiO_2 interface

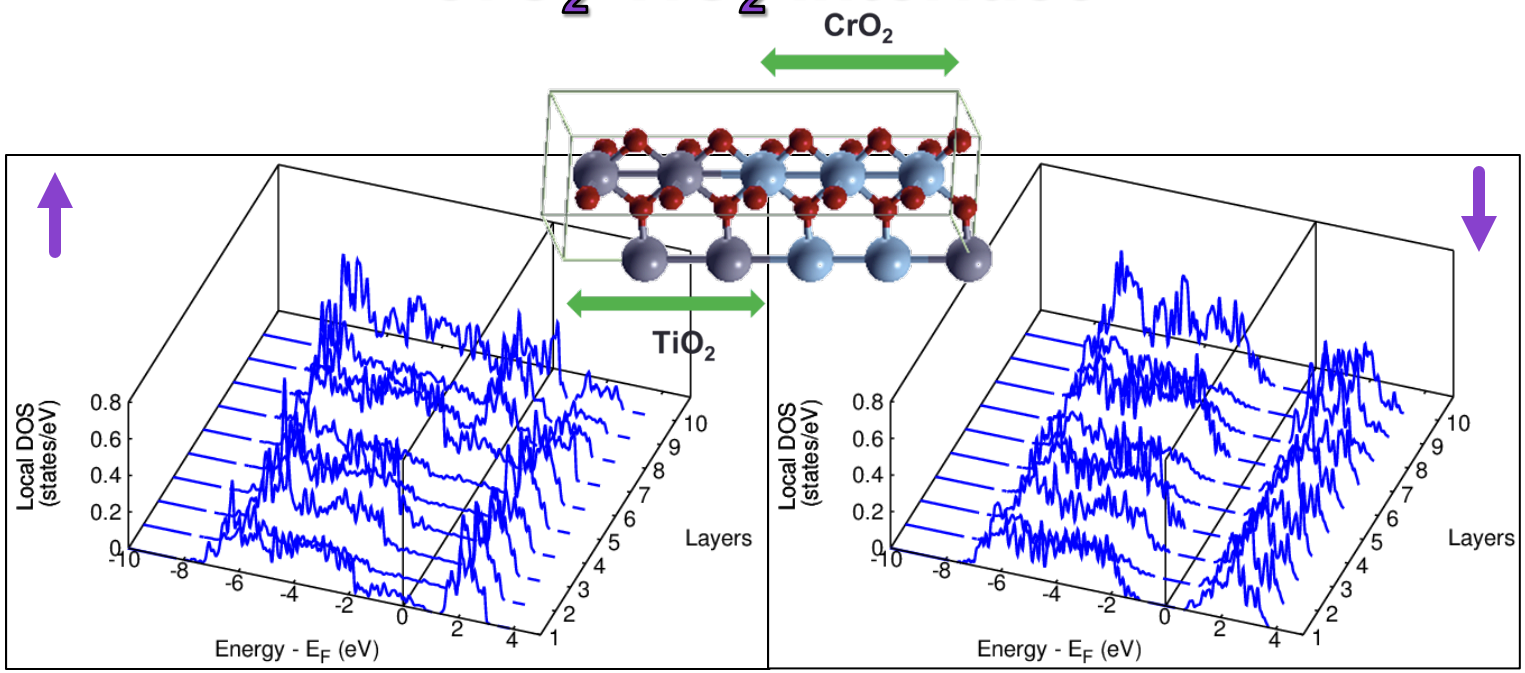

Possibility of tuning of band alignment
Shottky barrier *vs.* VBO

spin up SB	**1.09 eV**
spin dw VBO	**0.68 eV**

Ag O_2-TiO_2	**Hf** O_2-TiO_2	**Ni** O_2-TiO_2	**Ru** O_2-TiO_2	**Y** O_2-TiO_2
Au O_2-TiO_2	**Ir** O_2-TiO_2	**Os** O_2-TiO_2	**Sc** O_2-TiO_2	**Zn** O_2-TiO_2
Cd O_2-TiO_2	**La** O_2-TiO_2	**Pd** O_2-TiO_2	**Ta** O_2-TiO_2	**Zr** O_2-TiO_2
Co O_2-TiO_2	**Mn** O_2-TiO_2	**Pt** O_2-TiO_2	**Tc** O_2-TiO_2	
Cu O_2-TiO_2	**Mo** O_2-TiO_2	**Re** O_2-TiO_2	**V** O_2-TiO_2	
Fe O_2-TiO_2	**Nb** O_2-TiO_2	**Rh** O_2-TiO_2	**W** O_2-TiO_2	

Half-metallic oxides: the HT search

- High-throughput search for half metallic oxides within *AFLOWLIB.ORG*
- ICSD (17000) ➔ 4848 oxides ➔ 123 half-metals

Binary oxides

1. Cr1O1_ICSD_109296
2. Co1O1_ICSD_17013
3. O5V3_ICSD_15899
4. Cr1O2_ICSD_155832
5. Fe3O4_ICSD_92356
6. Cr1O2_ICSD_9423
7. Mo1O2_ICSD_99714

Ternary oxides

1. Cr1Gd1O4_ICSD_26982
2. Cr1O3Pr1_ICSD_28932
3. La1Mn1O3_ICSD_29119
4. La1O3V1_ICSD_28925
5. O3Pr1V1_ICSD_28927
6. O3Sr1V1_ICSD_88982
7. Al1Fe2O4_ICSD_76977
8. Al1O4V2_ICSD_60413
9. Al2Fe1O4_ICSD_56117
10. Al2Ni1O4_ICSD_608815

Ternary oxides (contd.)

11. Br6K2Os1_ICSD_26770
12. Cd1O4V2_ICSD_28961
13. Ce2O7Zr2_ICSD_154755
14. Cl6K2Os1_ICSD_26769
15. Co2Ge1O4_ICSD_21115
16. Co2O4Si1_ICSD_859
17. Cr2Ni1O4_ICSD_28835
18. Cu1Mn2O4_ICSD_27920
19. Fe1Ni2O4_ICSD_109150
20. Li1Mn2O4_ICSD_40485
21. Li1O2Ti1_ICSD_48128
22. Mg1O4V2_ICSD_56283
23. Mg2O4V1_ICSD_76980
24. Mn1O4Ti2_ICSD_22383
25. Mn1O4V2_ICSD_109148
26. Mo2O7Tb2_ICSD_159770
27. Mo2O7Y2_ICSD_202522
28. Nd2O7Sn2_ICSD_82958
29. Nd2O7Zr2_ICSD_62793
30. O4V2Zn1_ICSD_28963

Ternary oxides (contd.)

31. O7Pr2Sn2_ICSD_82957
32. Ag1Ni1O2_ICSD_415451
33. Fe2Na1O3_ICSD_200009
34. K3O8V3_ICSD_100782
35. Mn1Na2O4_ICSD_39504
36. B1Fe3O5_ICSD_25101
37. Co2O7P2_ICSD_74542
38. Cr1O5Ti2_ICSD_65219
39. O13V6_ICSD_15028
40. H1Mn1O2_ICSD_84948
41. La1Mn1O3_ICSD_16280
42. Al1O3Pr1_ICSD_35549
43. Al1O4V2_ICSD_151457
44. Ba3Cr2O8_ICSD_9457
45. Ce7O12_ICSD_88754
46. Cr2O8Sr3_ICSD_85055
47. Cu1O2Pr1_ICSD_18103
48. Er1Fe2O4_ICSD_67700
49. Fe2O4Y1_ICSD_67701
50. K1O2Pr1_ICSD_15157
51. La1Mn1O3_ICSD_55953
52. Li1Ni1O2_ICSD_26608
53. Ni1O3Pr1_ICSD_69186

Half-metallic oxides: the HT search

- High-throughput search for half metallic oxides within *AFLOWLIB.ORG*

Quaternary oxides

1. Mn7Na1O12_ICSD_19022
2. Ba2Ca1O6Os1_ICSD_171988
3. Ba2Co1O6W1_ICSD_27425
4. Ba2Dy1O6Re1_ICSD_25396
5. Ba2Fe1Mo1O6_ICSD_96688
6. Ba2Ho1O6Re1_ICSD_25397
7. Ba2La1O6Re1_ICSD_25392
8. Ba2Nb1Nd1O6_ICSD_109152
9. Ba2Nd1O6Sb1_ICSD_38328
10. Ba2O6Re1Tb1_ICSD_25395
11. Ba2O6Re1Y1_ICSD_94215
12. Co1Mo1O6Sr2_ICSD_28601
13. Co1O6Sr2W1_ICSD_28598
14. Cr1O1.01_ICSD_61633
15. Dy1O6Re1Sr2_ICSD_25402
16. Er1O6Re1Sr2_ICSD_25405
17. Fe1Mo1O6Sr2_ICSD_157603
18. Gd1O6Re1Sr2_ICSD_25400
19. Ho1O6Re1Sr2_ICSD_25403
20. O6Re1Sr2Tb1_ICSD_25401
21. O6Re1Sr2Y1_ICSD_25404
22. Ba1O11V6_ICSD_416450
23. Ca2Fe7O11_ICSD_100827
24. Co2Na3O6Sb1_ICSD_245538
25. O26V12_ICSD_16779
26. Ba2Nb1O6Pr1_ICSD_245457
27. Ca1Mn7O12_ICSD_200971
28. Co1K2O6Se2_ICSD_71536
29. Ba1Mn2Nd1O5_ICSD_158889
30. Ba1Mn2Nd1O6_ICSD_150705
31. Ba1Mn2O5Pr1_ICSD_158885
32. Ba1Mn2O5Y1_ICSD_83690
33. Ba1Mn2O5Y1_ICSD_88949
34. Cl1Mn1O3Sr2_ICSD_94745

Senary oxide

Al12Nd4O32Pb8_ICSD_406531

LARGE PHASE-SPACE

Quinary oxides

1. Cu3Dy1Mn4O12_ICSD_153871
2. Cu3Ho1Mn4O12_ICSD_153872
3. Cu3Mn4O12Y1_ICSD_38418
4. Na1O12P3V3_ICSD_202911
5. B6Ba2Co1O12_ICSD_391014
6. Mo2Na1O12P3_ICSD_202860
7. K1Na1O5Pr1Ta1_ICSD_419857
8. K1O5S2Ti2Y2_ICSD_96951

The search for functionality: Spinel half-metallic oxides

Perovskites

•**Ternary oxides**

- Cr1O3Pr1_ICSD_28932
- La1Mn1O3_ICSD_29119
- La1O3V1_ICSD_28925
- O3Pr1V1_ICSD_28927
- O3Sr1V1_ICSD_88982
- La1Mn1O3_ICSD_16280
- Al1O3Pr1_ICSD_35549
- Ni1O3Pr1_ICSD_

Spinels

Ternary oxides

- Cr1Gd1O4_ICSD_26982
- Al1Fe2O4_ICSD_76977
- Al1O4V2_ICSD_60413
- Al2Fe1O4_ICSD_56117
- Al2Ni1O4_ICSD_608815
- Cd1O4V2_ICSD_28961
- Co2Ge1O4_ICSD_21115
- Co2O4Si1_ICSD_859
- Cr2Ni1O4_ICSD_28835
- Cu1Mn2O4_ICSD_27920
- Fe1Ni2O4_ICSD_109150
- Li1Mn2O4_ICSD_40485
- Mg1O4V2_ICSD_56283
- Mg2O4V1_ICSD_76980
- Mn1O4Ti2_ICSD_22383
- Mn1O4V2_ICSD_109148
- O4V2Zn1_ICSD_28963
- Al1O4V2_ICSD_151457
- Er1Fe2O4_ICSD_67700

Pyrochlores

Ternary oxides

- Ce2O7Zr2_ICSD_154755
- Mo2O7Tb2_ICSD_159770
- Mo2O7Y2_ICSD_202522
- Nd2O7Sn2_ICSD_82958
- Nd2O7Zr2_ICSD_62793

The search for functionality: Spinel oxides

- 20 ternary oxides in the spinel structures found to be half-metallic
  - Normal spinel: A[2+]B[3+]O4
    - A → 8 (tetrahedral)
    - B → 16 (octahedral)
    - O → 32
  - Inverse spinel: (B)[A,B]O4
- Complex crystal structure offers many possibilities for materials design.
- Potential electronic/spintronic materials:
  - Interstitial doping
  - <u>Half-metals</u>

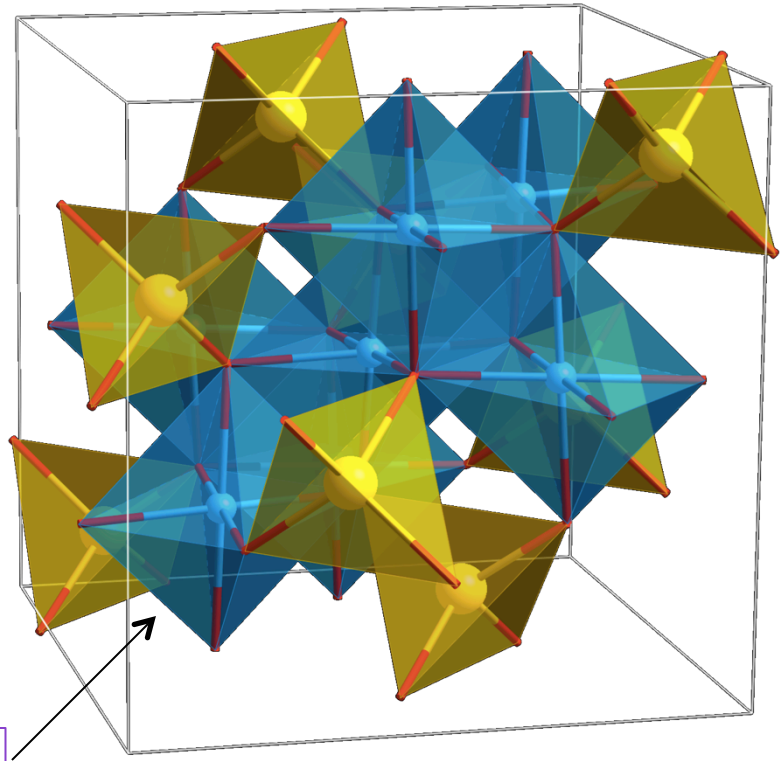

Edge-sharing oxygen octahedra

Materials design in spinel oxides

Relative structural stability

	E (normal) (eV)	E(inverse) (eV)	
CuAl2O4	-90.672	-93.872	Inv
NiAl2O4	-92.453	-94.937	inv
FeAl2O4	-105.019	-103.095	normal
CuMn2O4	-91.609	-91.242	normal
CuRh2O4	-72.308	-69.585	normal
GeCo2O4	-85.38	-87.063	inv
SiCo2O4	-95.302	In progress	
Ni2FeO4	-69.892	-71.828	inv
AlFe2O4	-98.912	-100.002	Inv
FeNi2O4	-78.321	-79.043	Inv
FeCr2O4	-106.017	In progress	
MnV2O4	-112.436	-111.990	normal
MnTi2O4	-124.144	-122.941	normal
NiCr2O4	-97.916	-98.491	Inv

Strain effect study in progress.

Acknowledgments

- *AFLOWLIB/*ONR-MURI team: S. Curtarolo, M. Buongiorno Nardelli, M. Fornari, G. Hart, R. Forcade, I. Takeuchi

- University of North Texas
  - **Luis Agapito**, research professor
  - Arrigo Calzolari (CNR-NANO-S3, Italy)

- University of North Texas/Central Michigan
  - **Priya Gopal**, post-doc
  - **Laalitha Lianage**, post-doc

- Duke
  - **K. Yang**, post-doc

http://ermes.unt.edu

http://www.quantum-espresso.org

http://QE-forge.org

http://AFLOWLIB.org